PLOS ONE

RESEARCH ARTICLE

Galleria mellonella as an insect model for *P. destructans*, the cause of White-nose Syndrome in bats

Chapman N. Beekman, Lauren Meckler, Eleanor Kim, Richard J. Bennett*

Department of Molecular Microbiology and Immunology, Brown University, Providence, RI United States of America

* Richard_Bennett@brown.edu

Check for updates

OPEN ACCESS

Citation: Beekman CN, Meckler L, Kim E, Bennett RJ (2018) *Galleria mellonella* as an insect model for *P. destructans*, the cause of White-nose Syndrome in bats. PLoS ONE 13(9): e0201915. https://doi.org/10.1371/journal.pone.0201915

Editor: Vishnu Chaturvedi, Wadsworth Center, UNITED STATES

Received: January 17, 2018

Accepted: July 24, 2018

Published: September 5, 2018

Copyright: © 2018 Beekman et al. This is an open access article distributed under the terms of the Creative Commons Attribution License, which permits unrestricted use, distribution, and reproduction in any medium, provided the original author and source are credited.

Data Availability Statement: All relevant data are within the paper and its Supporting Information files.

Funding: This work was funded by National Science Foundation (https://www.nsf.gov/) grant number 1456787 to RJB. The funders had no role in study design, data collection and analysis, decision to publish, or preparation of the manuscript.

Competing interests: The authors have declared that no competing interests exist.

Abstract

Pseudogymnoascus destructans is the fungal pathogen responsible for White-nose Syndrome (WNS), a disease that has killed millions of bats in North America over the last decade. A major obstacle to research on *P. destructans* has been the lack of a tractable infection model for monitoring virulence. Here, we establish a high-throughput model of infection using larvae of *Galleria mellonella*, an invertebrate used to study host-pathogen interactions for a wide range of microbial species. We demonstrate that *P. destructans* can kill *G. mellonella* larvae in an inoculum-dependent manner when infected larvae are housed at 13˚C or 18˚C. Larval killing is an active process, as heat-killed *P. destructans* spores caused significantly decreased levels of larval death compared to live spores. We also show that fungal spores that were germinated prior to inoculation were able to kill larvae 3–4 times faster than non-germinated spores. Lastly, we identified chemical inhibitors of *P. destructans* and used *G. mellonella* to evaluate these inhibitors for their ability to reduce virulence. We demonstrate that amphotericin B can effectively block larval killing by *P. destructans* and thereby establish that this infection model can be used to screen biocontrol agents against this fungal pathogen.

Introduction

Pseudogymnoascus destructans is the fungal species responsible for White-nose Syndrome (WNS), a disease currently devastating bat populations across North America. *P. destructans* is a psychrophilic fungus and colonizes susceptible bat species during hibernation, causing depletion of energy stores and death of the host. Since it was first discovered in New York State in 2006, WNS has spread to 32 US states and 5 Canadian provinces [1]. This rapid spread, combined with a mortality rate approaching 100% for several species, has led to an estimated 6 million bats being killed by WNS [1]. As a result, one of the most common bat species in the North-East US, the little brown bat (*Myotis lucifugus*), is now threatened with regional extinction. The loss of bats can harm both local ecosystems and agriculture as they play a crucial role in controlling insect pest populations, and it has been estimated that bat populations lost to WNS could cost the agricultural industry as much as $23 billion per year [2].

Despite the impact of WNS, a clear understanding of the factors that allow *P. destructans* to infect its host remain elusive. Studies have suggested several attributes may be important for

fungal virulence including the production of small molecule effectors [3], protease secretion [4, 5], lipid utilization [6], as well as the fungal heat shock response, cell wall remodeling, and micronutrient acquisition [7]. A significant obstacle to evaluation of these hypotheses has been the lack of a tractable infection model. The psychrophilic nature of *P. destructans* (maximum growth temperature of ~18 ˚C) has made standard mammalian infection models unfeasible. Laboratory-based WNS models using live bats have been utilized [8, 9], but require specialized equipment and long infection timelines, and are impractical for high-throughput studies.

The lack of an accessible infection model for *P. destructans* has also limited the testing of therapeutic agents to treat WNS. Studies have identified several agents that can inhibit *P. destructans* growth on laboratory media [10–12], yet these are difficult to test in a natural setting. Treating a live infection entails additional complications that are not present during growth on laboratory media, such as host drug toxicity or drug degradation by the host. Additionally, available carbon sources and growth conditions can affect fungal drug susceptibility [13, 14]. Treatment of WNS also poses unique challenges given that infection occurs only in hibernating bat populations, often located in remote habitats. Development of a simple host model of *P. destructans* infection would therefore be of considerable value and could accelerate the identification of an effective treatment for WNS.

For several fungal pathogens, larvae of the greater wax moth, *Galleria mellonella*, have provided a simple yet effective alternative to mammalian infection models. *G. mellonella* has been employed to study virulence in human fungal pathogens including *Candida* [15–17], *Aspergillus* [18, 19] and *Fusarium* [20, 21] species. Importantly, many results obtained using *G. mellonella* reproduce findings from mammalian infection studies [15, 19, 21, 22], indicating that larval infection shows parallels with that in higher eukaryotes. Though insects lack an adaptive immune system, their immune response closely resembles the mammalian innate immune response at both a structural and functional level [23]. *G. mellonella* hemocytes are functionally analogous to mammalian phagocytes and generate reactive oxygen species (ROS) for microbial killing [24, 25]. These features make *G. mellonella* a relevant model for WNS, as evidence suggests hibernating bats can mount an innate immune response to *P. destructans* but are unable to activate adaptive immunity [26–28]. To our knowledge, no previous studies using *G. mellonella* have been conducted at temperatures below 20˚C, yet larvae can be maintained at such temperatures making their use as a *P. destructans* infection model an attractive possibility.

Here, we examine the feasibility of using *G. mellonella* larvae as an invertebrate model for infection with *P. destructans*. Our results indicate that live *P. destructans* spores, but not heat-killed spores, are lethal to *G. mellonella* larvae, and that killing is augmented if spores are induced to germinate prior to inoculation. We also perform a screen to identify chemical inhibitors of *P. destructans* growth and evaluate their efficacy during infection. These experiments establish that insect larvae can be used as a high-throughput model for *P. destructans* enabling the screening of potential treatments for WNS.

Materials and methods

Strains and culture conditions

Pseudogymnoascus destructans strain 20631–21 (ATCC stock: MYA-4855) was used for all experiments. *P. destructans* cultures were cultured on yeast extract-peptone-dextrose (YPD) medium at 13˚C prior to spore collection.

G. mellonella virulence assays

G. mellonella larvae were obtained from Vanderhorst Wholesale (St. Marys, OH). Prior to infection, larvae were stored at 13˚C and used within 1 week of delivery. For all experiments,

inoculums were prepared by harvesting *P. destructans* spores from 2–3 week-old cultures grown on YPD plates using a solution of 0.05% Tween-20 (Sigma) and rubbing the surface of the plates with a glass spreader to release spores. Spores were isolated from larger hyphae by filtering through a layer of sterile miracloth, centrifuged and resuspended in 5 mL sterile phosphate-buffered saline, pH 7.4 (PBS). Spores were counted on a light microscope (Leica DM750) using a hemocytometer and adjusted to the desired concentration. Heat-killed spores were prepared by incubating inoculums for at least 30 min at 65˚C and re-cooling briefly on ice prior to injection. Efficacy of heat killing was confirmed by plating 1000 spores/plate on YPD and checking for viable colonies. For pre-germination experiments, *P. destructans* spores were adjusted to $1x10^7$ cells/mL in liquid YPD and incubated at 13˚C in a shaking incubator (200 rpm) for the specified time period. Spore germination was assessed by microscopic analysis of germ tubes versus un-germinated spores. Approximately 400 spores were counted in two independent experiments. Inoculums were then prepared by adjusting spores to $1x10^8$ cells/mL in sterile PBS. Larvae of similar size were randomly selected for each experiment and those showing discoloration were discarded. Each worm was injected with 10 μL of inoculating solution just below the second to last left proleg using a 10 μL glass syringe with a 26S gauge needle (Hamilton, 80300). Infected larvae and controls were maintained at 13˚C and checked daily. Larvae were recorded as dead if no movement was observed upon contact. For antifungal experiments, *P. destructans* spores were germinated for 6 h in YPD then either (1) resuspended in each compound in PBS for 2 hours or less prior to injection, or (2) compounds were applied to larvae 2 hours post-infection by a second 10 μL injection at the last right proleg. Control larvae for these latter experiments received a second injection containing only PBS.

Histology

Larvae were injected with 12 h-germinated *P. destructans* spores or an equal volume of PBS as described above and incubated at 13˚C. At 1, 2 and 3 weeks post-infection, larvae were removed and injected with 100 uL of 4% paraformaldehyde using an insulin syringe, submerged in 2 mL of the fixative solution and incubated for 3 days at 4˚C to allow complete fixation. Fixed larvae were then cut into 4–5 segments using a scalpel, embedded in paraffin and sectioned at 5 μm using a Leica EG1150C microtome. Sections were stained using Modified Grocott's Methanamine Silver (GMS) Stain (Thermo, #87008) and imaged by light microscopy (Leica DM750).

Colony forming units (CFUs) in infected larvae

Larvae were injected with 12 h-germinated live or heat-killed *P. destructans* spores and incubated at 13˚C. At 1, 2 and 3 weeks, infected larvae were removed, weighed and placed on ice for 5–10 minutes to immobilize. Larvae were then homogenized in PBS containing kanamycin (110 μg/mL), doxycycline (250 μg/mL), penicillin (1 mg/mL) and streptomycin (500 μg/ml) by slicing into small segments with a scalpel and grinding with a plastic syringe plunger against a cell strainer (70 μm, Fisher) contained within a 6-well tissue culture plate. Each larval homogenate was plated neat and as 1:100 dilutions on YPD plates and plates were counted for *P. destructans* colonies after 8–10 days at 13˚C.

Phenotype Microarray (PM) screen

P. destructans spores were harvested, washed in PBS, counted, and adjusted to $1x10^6$ cells/mL in YPD. Next, 100 μL of the spore solution was used to inoculate each well of PM plates 21–25 (Biolog, Hayward, CA). Each well contains one of 120 different chemical compounds at 4 different concentrations [29]. Plates were incubated at 13˚C and growth in each well was

monitored daily by measuring optical density (OD595 nm) in a Synergy HT plate reader (Biotek, Winooski, VT) for 11 days. OD readings were compiled to construct growth curves which were analyzed using DuctApe™ software [30] to convert each growth curve into an "activity index" (0–9) representing relative growth of *P. destructans* in response to each chemical. Data shown represents the average activity indices from 2 independent experiments.

Comparison of *P. destructans* and *C. albicans* PM data

Data from the PM drug screen on *P. destructans* was compared with published data obtained for *C. albicans* using the same PM drug panel and DuctApe analysis software [31]. Inhibitory compounds were defined as those producing an activity index of 0 at any concentration. Individual compounds were compared using the BioVenn [32] webtool. Compounds were categorized by "mode of action" and each category was evaluated for enrichment of inhibitory compounds (Fishers exact test, Graphpad Prism v.5).

Determination of minimum inhibitory concentrations (MICs)

P. destructans spores were harvested and adjusted to $1x10^6$ spores/mL in YPD solutions containing test compounds. These solutions were then used to inoculate individual wells of clear plastic 96-well tissue culture plates (100 μL/well, 6 replicate wells/condition). Plates were incubated at 13˚C and growth (OD595) measured after 240 h using a Synergy HT plate reader (Biotek). OD values from each of the 6 replicate wells were averaged and then divided by the average growth in control wells containing spores in YPD to determine the fraction of growth. The MIC was defined as the lowest concentration of each compound able to reduce *P. destructans* growth by at least 80%.

Evaluation of compounds for fungicidal activity

Harvested *P. destructans* spores were adjusted to $1x10^6$ spores/mL in YPD containing the test compound and incubated at 13˚C for 24 h. Next, serial dilutions of the spore solutions were made in YPD and 2 μL of each dilution spotted onto YPD plates, incubated at 13˚C for 1 week and imaged using a Chemidoc imaging system (BioRad).

Results

Evaluation of *G. mellonella* as a suitable host for *P. destructans*

To test if *P. destructans* can establish an infection in *G. mellonella*, larvae were injected with 10^4, 10^5, or 10^6 fungal spores in phosphate-buffered saline (PBS) or mock infected with PBS alone. Injected larvae were incubated at either 13˚C or 18˚C as appropriate temperatures for growth of *P. destructans*. At 18˚C, the upper limit for growth of *P. destructans*, increased inoculum size correlated with increased killing of *Galleria* larvae (Fig 1A). In contrast, at 13˚C, only the highest inoculum of 10^6 spores per larva demonstrated increased lethality above the PBS-injected control group ($p = 0.0167$, log-rank test, Fig 1B). At the highest inoculum, the rate of killing was similar at both 13˚C and 18˚C, with 50% mortality reached ~20–25 days after infection. Larvae injected with the highest fungal inoculum also showed an increase in pigmentation within 2 weeks of injection at both temperatures (Fig 1C). Increased pigmentation in *Galleria* is likely due to melanization of host tissues, and is indicative of an immune response to infectious agents [33]. Less pigmentation was observed in larvae that received smaller inoculums (10^4 or 10^5 spores) and was completely absent in PBS-injected controls. Thus, pigmentation was a specific response to fungal spores and not due to physical injury caused by the injection. At 18˚C, several larvae appeared to form pupae while no pupae were observed at

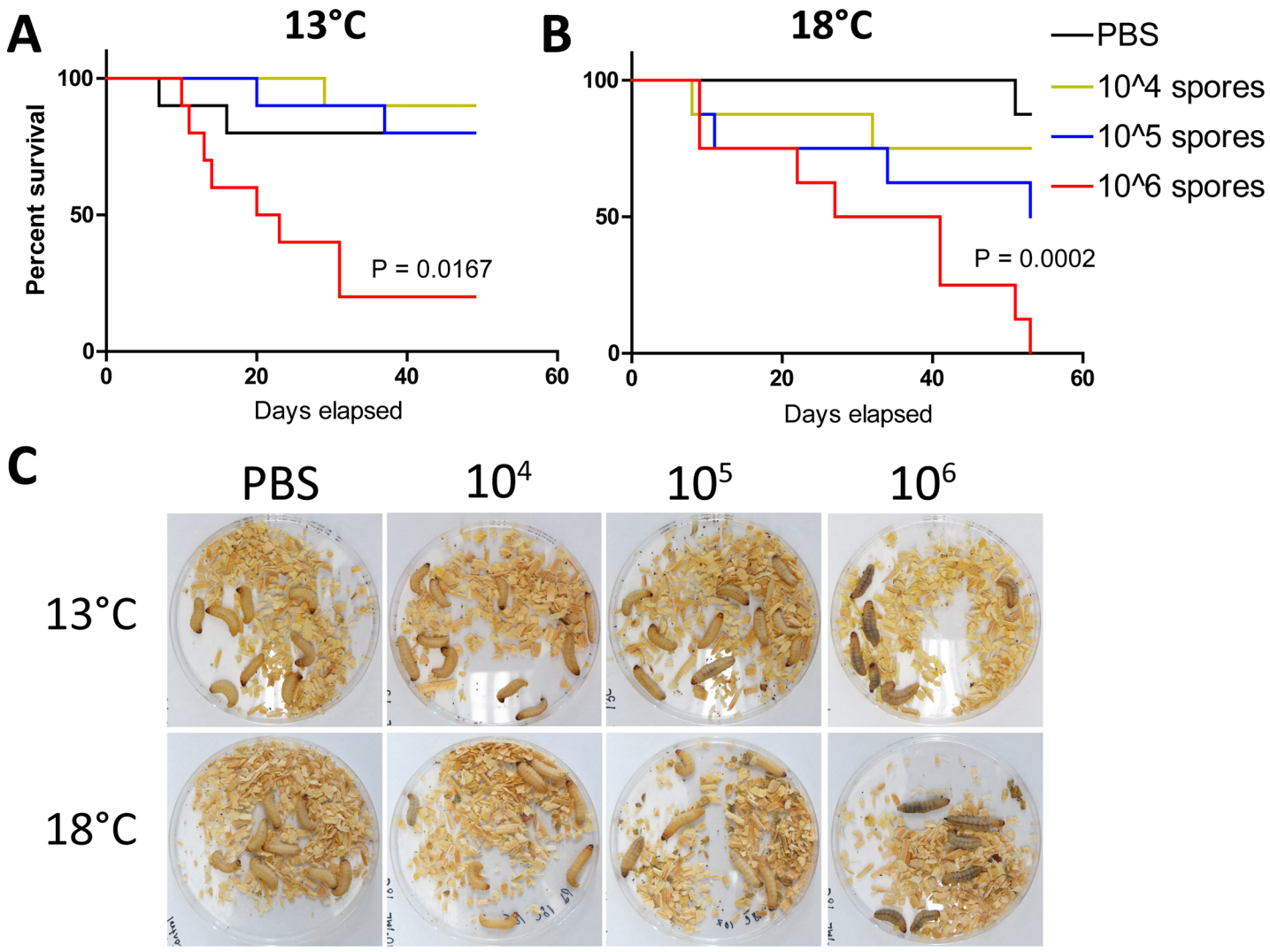

Fig 1. Inoculation of *G. mellonella* larvae with *P. destructans* spores leads to larval killing in an inoculum- and temperature-dependent manner. (A,B) 10 larvae each were injected with 10^4, 10^5 or 10^6 spores or an equal volume of PBS (control) and kept at 13˚C (A) or 18˚C (B). Larvae were monitored daily and deaths recorded. p-values represent Log-rank test in infections with 10^6 spores v. PBS control. (C) Images of infected larvae 16 days post-inoculation. Melanization can be seen in infected larvae and increases with inoculum size.

https://doi.org/10.1371/journal.pone.0201915.g001

13˚C for the duration of the experiment. To avoid potential impacts of pupation on larval survival, all subsequent experiments were conducted at 13˚C.

Lethal infections require live spores

The killing of *G. mellonella* by *P. destructans* spores could be due to active proliferation of fungal cells in the larvae, or due to the host response to spores regardless of whether the spores were viable. To distinguish between these possibilities, heat-killed spores were prepared by treatment at 65˚C for 30 minutes. Plating of heat-treated spores onto YPD medium established that less than 0.1% of spores were viable (Fig 2A, inset). Heat-killed and live spores were used to infect *G. mellonella* and larval death was monitored daily. While some mortality was observed in larvae infected with heat-killed spores, live *P. destructans* spores caused significantly greater killing of the larvae ($P < 0.0001$) (Fig 2A). Histology demonstrated a substantial

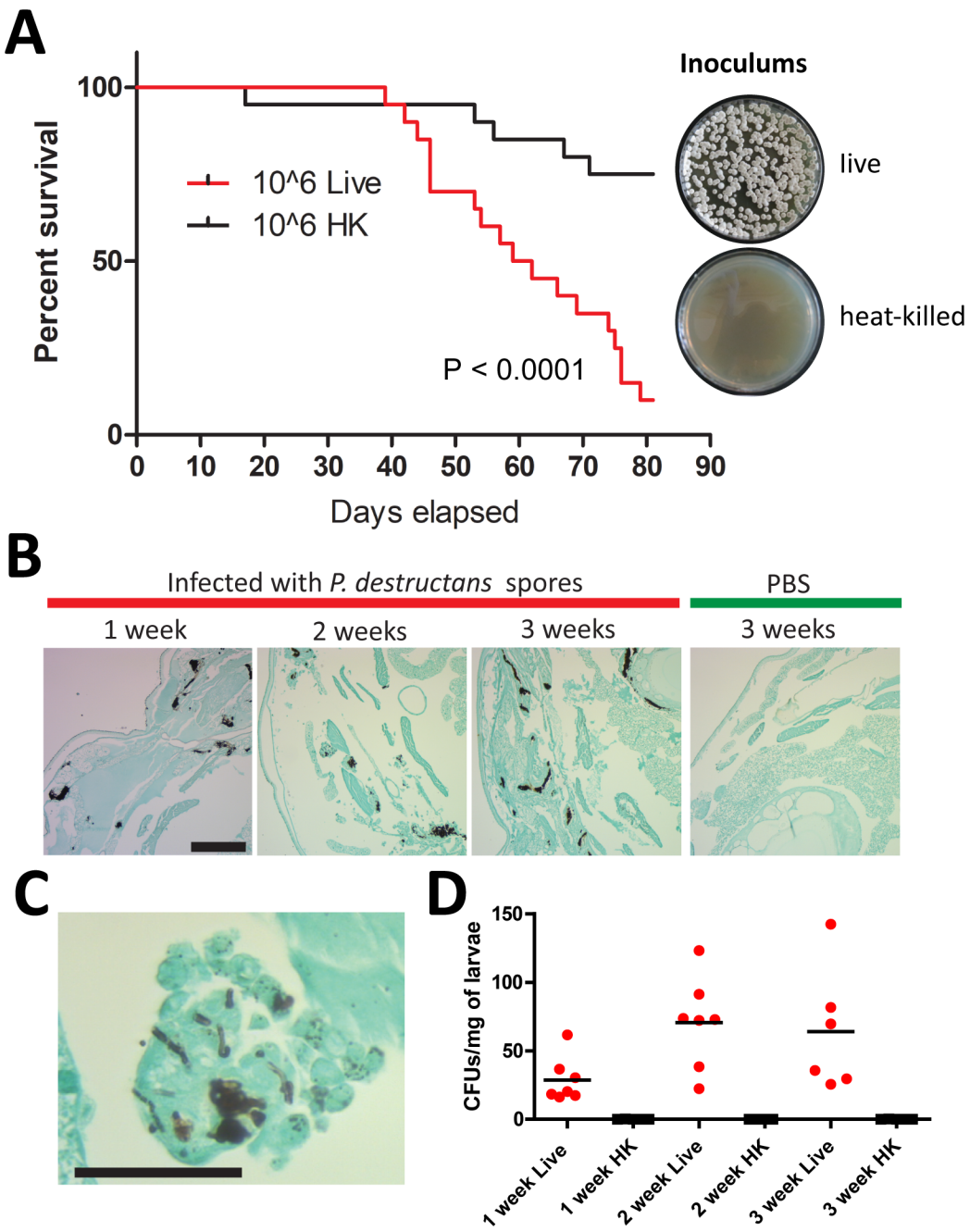

Fig 2. Effective killing of larvae requires live *P. destructans* spores. (A) Larvae were injected with 10^6 live spores or an equal number of heat-killed (HK) spores, kept at 13˚C and monitored daily. 20 larvae were used per condition in two independent experiments, p-value represents result of Log-rank test on Live vs. HK. Right inset: representative YPD agar plates on which 1000 spores from live and heat-killed inoculums were plated to confirm efficacy of heat-killing. (B) histology of larval tissues injected with live 12 h-germinated *P. destructans* spores (red bar) or mock-infected (green bar) and fixed 1, 2 or 3 weeks post-infection. Fungal elements were visualized using modified Grocott's Silver Stain (GMS) and light microscopy (10x magnification, scale bar = 200 μm). (C) Histology of infected larval tissue 2 weeks after infection with live 12 h-germinated *P. destructans* spores, stained with modified GMS and imaged by light microscopy (40x, scale bar = 50 μm). (D) CFUs indicating *P. destructans* colonies recovered from larvae infected with 12 h-germinated live (red dots) or heat-killed (HK, black squares) spores. Data points represent individual larvae.

https://doi.org/10.1371/journal.pone.0201915.g002

fungal burden within larval tissue after infection (Fig 2B), with many hyphal forms of *P. destructans* observed (Fig 2C). Counts of colony-forming units (CFUs) were also conducted and showed that CFUs (normalized by larval weight) increased during the first 2 weeks of infection with an average of 29 CFUs/mg, 71 CFUs/mg and 64 CFUs/mg detected after 1,2, or 3 weeks, respectively. Together, these results indicate the proliferation of *P. destructans* cells and the formation of hyphal filaments within larval tissue, and are consistent with active fungal growth leading to larval killing.

Virulence of *P. destructans* is increased by pre-germinating fungal spores

We examined whether spore germination could have an impact on the survival times of larvae. *P. destructans* spores were harvested and incubated at 13˚C in liquid YPD medium for varying amounts of time to allow germination prior to infection of *G. mellonella*. Spores were cultured for 0, 6, 12 or 24 hours in YPD and microscopic examination revealed that germ tube formation was clearly visible in those grown for 12–24 hours (Fig 3A). The extent of germination in each of the inoculums was calculated by counting spores with visible germ tubes versus non-germinated spores. We found that ~50% of spores incubated for 24 h in YPD had formed germ tubes and many cells had already formed hyphae (Fig 3A and 3B). This contrasts with ~35% of spores having germinated after 12 h in YPD, while at 0 h or 6 h less than 10% of spores had visible germ tubes.

Germinated *P. destructans* spores were found to kill larvae much more rapidly than non-germinated spores. Live spores that had been pre-incubated for 24 hours at 13˚C killed 50% of infected larvae within ~10 days, whereas larvae injected with spores germinated for 0, 6 or 12 h reached 50% mortality at approximately 45 days, 20 days or 15 days, respectively (Fig 3C). Increased melanization was also observed in larvae infected with spores that were pre-germinated (both live and heat-killed), indicating that germinated spores may elicit a stronger immune response from the host (Fig 3D). However, the increased melanization did not directly impact mortality rates as germinated heat-killed spores still produced little death in the host.

Antifungal drug screen with Phenotype Microarray (PM) plates

We next examined the feasibility of using *G. mellonella* larvae for evaluating antifungal agents against *P. destructans*. An *in vitro* screen was conducted to identify chemical inhibitors of *P. destructans* using the Phenotype Microarray (PM) system (Biolog) which consists of 96 well plates (PM21-25) coated with a panel of 120 chemical compounds at 4 different concentrations (for a full list of compounds see S1 Table)[29]. *P. destructans* spores suspended in YPD were used to inoculate each PM well and growth was monitored over the course of 11 days by measuring optical density (OD595). The resulting growth curves were analyzed using DuctApe software to generate an "activity index" representing relative fungal growth in the presence of a given compound (0 = no growth to 9 = maximal growth)[30]. Of the 120 compounds tested, approximately one third (42/120) were able to fully inhibit growth of *P. destructans* (activity index = 0) under at least one of the concentrations tested (Fig 4A). The compounds that were able to fully inhibit growth are predicted to act on a wide range of cellular targets including the cell membrane, cell wall, protein synthesis and cellular respiration (Fig 4B, S1 Table). However, two prominent classes of inhibitory compounds included those targeting the cell membrane ($p < 0.0001$, Fisher's exact test) and antipsychotics/efflux pump inhibitors ($p = 0.0136$), suggesting that these may represent aspects of *P. destructans* biology that are particularly sensitive to perturbation.

The sensitivity of *P. destructans* to chemical inhibitors was compared to that of the human fungal pathogen, *Candida albicans*, which was previously evaluated in PM plate assays (Fig 4B,

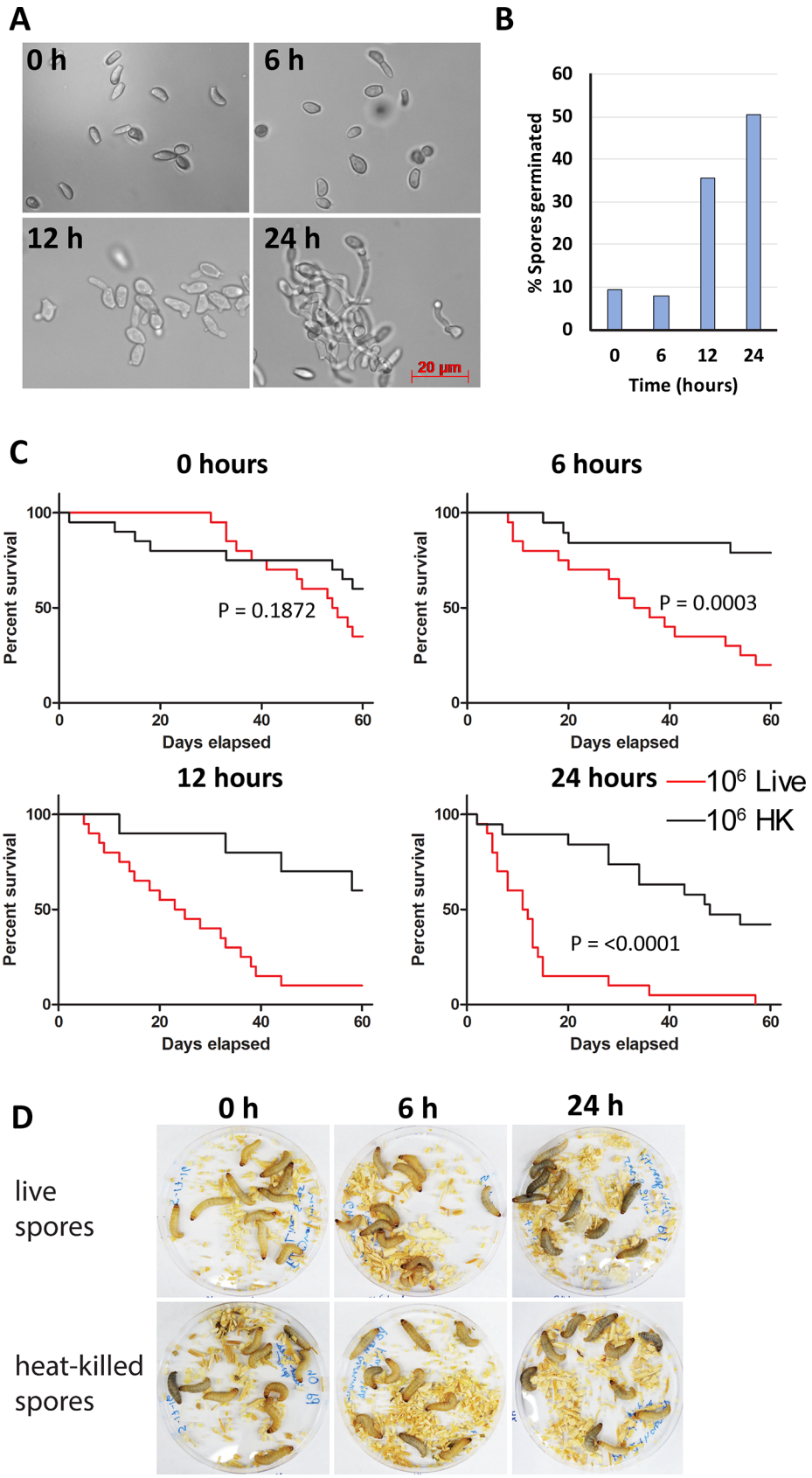
A
0 h
6 h
12 h
24 h
20 µm
B
% Spores germinated
0
10
20
30
40
50
60
0
6
12
24
Time (hours)
C
0 hours
6 hours
12 hours
24 hours
Percent survival
Days elapsed
P = 0.1872
P = 0.0003
P = <0.0001
10^6 Live
10^6 HK
D
0 h
6 h
24 h
live spores
heat-killed spores

Fig 3. Pre-germinated *P. destructans* spores kill larvae more effectively than non-germinated spores. (A) Representative images of inoculums demonstrate formation of germ tubes by fungal spores after 12 and 24 h in YPD. (B) Quantification of germ tube formation at each time point. Data represents analysis of > = 400 spores from two independent experiments for each time-point. (C) Larvae were each injected with either 10^6 live or heat-killed (HK) spores which had been allowed to pre-germinate for 0, 6, 12 or 24 h. Larval deaths were recorded daily. 20 larvae from two independent experiments were used per condition. p-values represent results of Log-rank test on live v. HK spores. (D) Images of larvae infected with spores allowed to germinate for 0, 6, or 24 h (images taken 2 h post-infection) shows greatest melanization in larvae infected with spores pre-germinated for 24 h.

https://doi.org/10.1371/journal.pone.0201915.g003

orange bars [31]). *C. albicans* cells similarly showed a significant enrichment for inhibitory compounds targeting the cell membrane (p = 0.0260). Additionally, all four of the compounds annotated as efflux pump inhibitors within the PM panel (trifluoperazine, thioridazine, promethazine and chlorpromazine) were able to fully inhibit growth of both *P. destructans* and *C. albicans*. This indicates that the sensitivity of *P. destructans* to compounds targeting the cellular membrane and efflux pumps is not unique among fungal pathogens. This comparison also revealed that *P. destructans* was sensitive to a smaller number of PM compounds than *C. albicans* (42 and 68 compounds, respectively, Fig 4C). Only 5 inhibitory compounds were unique to *P. destructans* and these were benzamidine, cadmium chloride, ceftriaxone, sodium azide and sodium thiosulfate. This may indicate that *P. destructans* is generally more resistant to chemical inhibitors than *C. albicans*, although the growth media differed between these two studies which limits direct comparisons between the two species.

Evaluation of PM drug screen hits

A subset of the 42 inhibitory compounds identified from the PM screen were selected for further evaluation. Compounds known to possess high toxicity toward animal species were avoided. For each test compound, the minimum inhibitory concentration (MIC) was determined by testing a range of drug concentrations against *P. destructans* grown in YPD using the broth dilution method. The MIC of each compound was defined as the minimum concentration at which at least 80% of fungal growth was inhibited. The majority of compounds tested showed MICs within the millimolar range, however two compounds, trifluoperazine and sodium thiosulfate, had MICs in the micromolar range (130 μM or 53 μg/mL and 12.5 μM or 2 μg/mL, respectively) indicating they are relatively potent inhibitors of *P. destructans* growth (Table 1).

Each test compound was also evaluated to determine if it was fungistatic or fungicidal. To determine fungicidal activity, *P. destructans* spores were exposed to test compounds at a concentration 10-fold higher than the determined MIC for 24 h and plated onto YPD to assess their viability (Fig 4D). A compound was considered fungicidal if *P. destructans* was unable to grow on YPD plates after exposure. Of the compounds tested, only trifluoperazine showed fungicidal activity whereas all other compounds appeared fungistatic.

Inhibitory compounds can block killing of *G. mellonella* larvae by *P. destructans*

Trifluoperazine and sodium thiosulfate, the most potent inhibitors of *P. destructans* identified *in vitro*, were tested for their ability to block killing of *G. mellonella* larvae. Two widely used antifungal drugs, amphotericin B and fluconazole [34], were also tested in these experiments. We note that *P. destructans* has previously been shown to be susceptible to fluconazole in a dose-dependent manner [10], while amphotericin B fully inhibited *P. destructans* growth under 3 of 4 concentrations tested in the Biolog screen. For each assay, *P. destructans* spores were harvested, pre-germinated, resuspended in PBS containing the test compound and

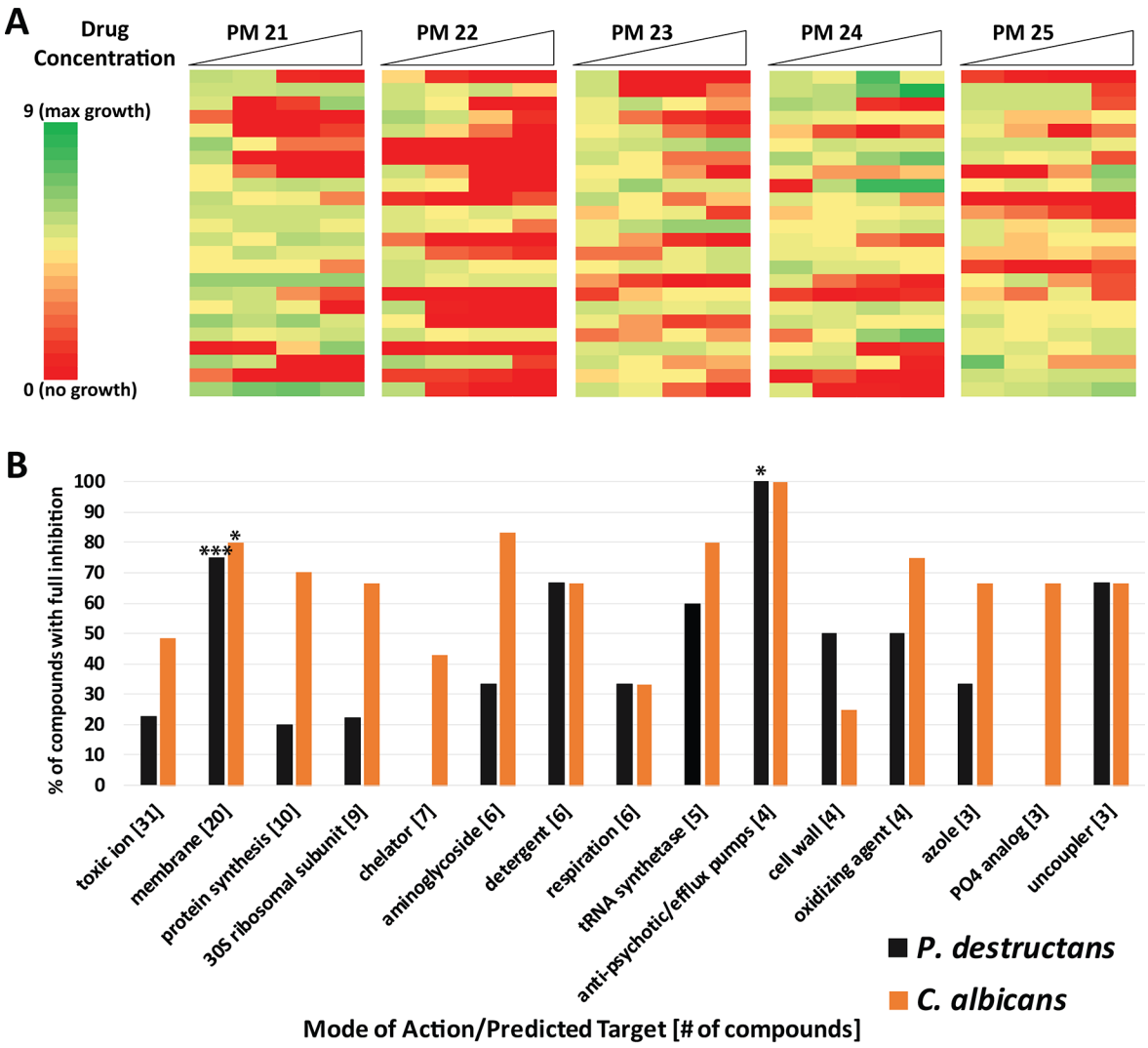
A
Drug Concentration
PM 21
PM 22
PM 23
PM 24
PM 25
9 (max growth)
0 (no growth)
B
% of compounds with full inhibition
100
90
80
70
60
50
40
30
20
10
0
***
*
*
toxic ion [31]
membrane [20]
protein synthesis [10]
30S ribosomal subunit [9]
chelator [7]
aminoglycoside [6]
detergent [6]
respiration [6]
tRNA synthetase [5]
anti-psychotic/efflux pumps [4]
cell wall [4]
oxidizing agent [4]
azole [3]
PO4 analog [3]
uncoupler [3]
P. destructans
C. albicans
Mode of Action/Predicted Target [# of compounds]
C
42
Unique to
P. destructans
(5)
Shared (37)
Unique to
C. albicans (31)
68
D
Pd cells: 2 x ... 10^3 10^2 10^1 10^0
Control (YPD, no drug)
Benzamidine
Boric Acid
Caffiene
Sod. Thiosulfate
Ferulic acid
Sod. Octanoate
Isoniazid
Trifluoperazine

Fig 4. Identification and evaluation of anti-*P. destructans* compounds. (A) Heat map representing relative *P. destructans* growth on PM plates 21–25 which contain a total of 120 test compounds. (B) Bar graph indicating the % of PM compounds within each mode of action/target category that were able to fully inhibit growth of *P. destructans* (black) or *C. albicans* (orange) * P < = 0.05, *** P < = 0.001 (Fisher's exact test). (C) Venn-diagram indicating compounds able to inhibit *P. destructans* and *C. albicans* growth. (D) Images of *P. destructans* spores spotted onto YPD agar as 10-fold dilutions from left (10^3) to right (10^0) and allowed to grow for 1 week after an initial 24 h exposure to the indicated compound at 10 times the MIC concentration.

https://doi.org/10.1371/journal.pone.0201915.g004

injected into *Galleria* larvae alongside controls (spores in PBS alone). Treatment of spores with sodium thiosulfate or fluconazole failed to reduce larval killing compared to infections with untreated spores (Fig 5A and 5B). However, both trifluoperazine and amphotericin B blocked larval killing by *P. destructans*, reducing the rate of mortality to that produced by heat-killed spores ($p < 0.0001$, log-rank test, Fig 5C and 5D). In these experiments, untreated spores killed 50% of larvae after 20 days and 100% of larvae by 42 days, whereas >90% of larvae inoculated with trifluoperazine-treated spores and 65% of larvae inoculated with amphotericin B-treated spores were still viable 60 days post-infection.

Amphotericin B and trifluoperazine were also tested for their efficacy as treatments post infection. However, when each compound was injected 2 hours after infection only amphotericin B significantly reduced larval killing (Fig 6A), while trifluoperazine showed no protection against *P. destructans* (Fig 6B). Thus, whereas 50% of larvae infected with live spores were killed within 22 days (and with less than 10% of larvae surviving to 60 days), over 50% of larvae treated with amphotericin B survived for 60 days or more.

Overall, these experiments demonstrate the utility of the *Galleria* model for the evaluation of *P. destructans* inhibitors and provide a proof-of-principle for screening of potential WNS treatments through the validation of amphotericin B as an *in vivo* inhibitor of pathogenesis.

Discussion

In this work, we establish the invertebrate *Galleria mellonella* as a suitable model for examining the virulence of *P. destructans*, the pathogen responsible for WNS. Our experiments demonstrate that *G. mellonella* larvae are susceptible to *P. destructans* at temperatures compatible with the growth of this fungus (13˚C or 18˚C). To our knowledge, this is the first evidence that the virulence of cold-loving, psychrophilic species can be studied in *G. mellonella*. Infection with *P. destructans* proceeds slowly, with larvae typically succumbing to infection over the course of 1–2 months. This time-frame is similar to infections of hibernating bats, where WNS gradually leads to progressive tissue damage and depletion of host reserves [8, 9].

P. destructans caused larval killing in an inoculum-dependent manner, with the most effective inoculum being 10^6 spores per larva. These inoculums are similar to those described for

Table 1. Selected anti-*P. destructans* compounds from PM drug screen.

Chemical	Mode of Action	MIC value (80% inhibition)
Caffeine	cyclic AMP phosphodiesterase inhibitor	**8 mM**
Boric acid	toxic anion	**25 mM**
Benzamidine	peptidase inhibitor, fungicide	**25 mM**
Trifluoperazine	membrane, phenothiazine, efflux pump inhibitor, anti-psychotic	**130 μM**
Sodium Thiosulfate	toxic anion, reducing agent	**12.5 μM**
Ferulic acid	antioxidant	**6 mM**
Sodium Caprylate	respiration, ionophore, H+	**50 mM**
Isoniazid	inhibitor of fatty acid synthesis	**50 mM**

https://doi.org/10.1371/journal.pone.0201915.t001

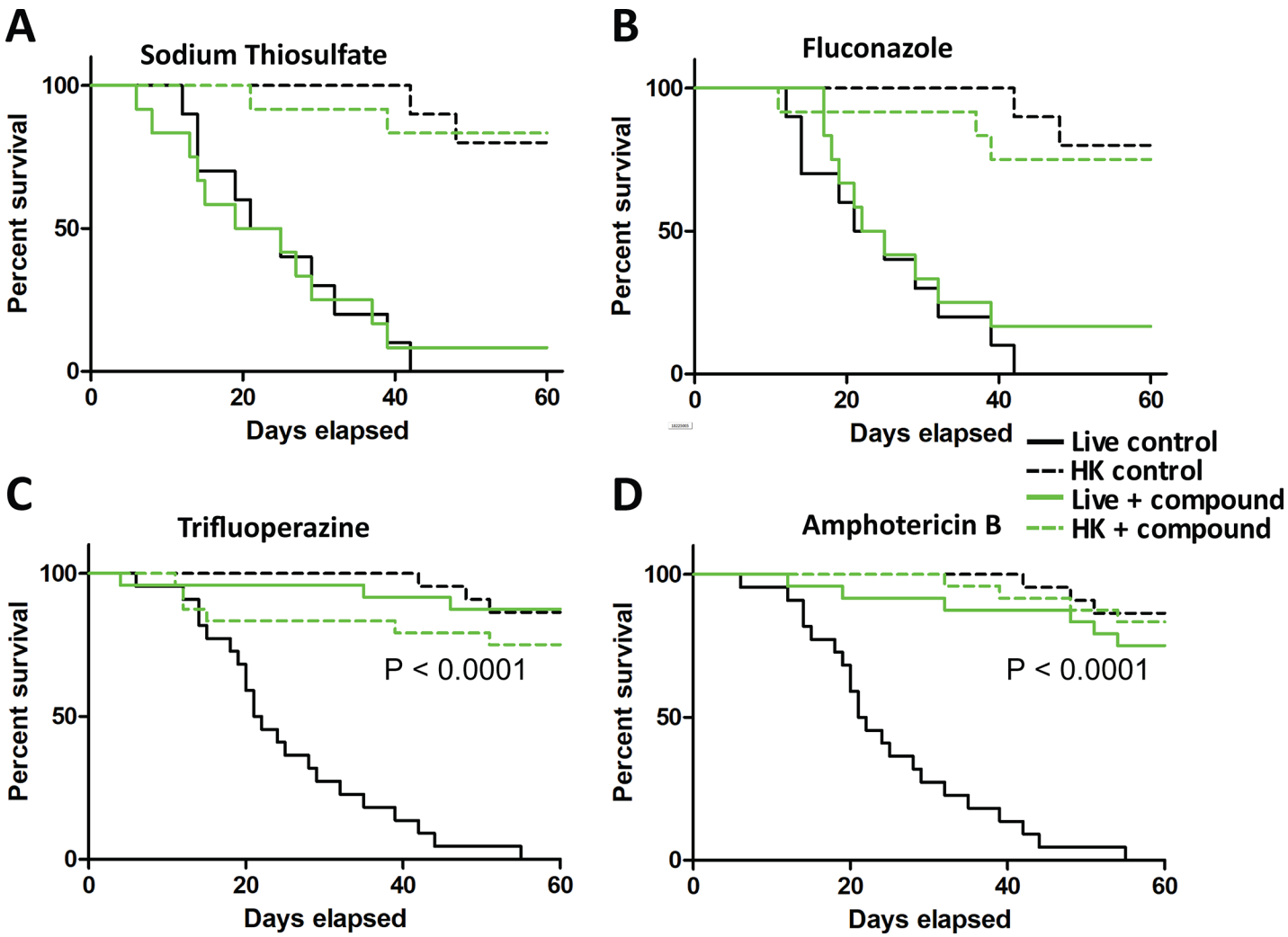

Fig 5. Evaluation of anti-*P. destructans* compounds using the *G. mellonella* infection model. Survival curves from *Galleria* larvae injected with spores (10^6/larva) resuspended in PBS containing sodium thiosulfate (125 μM) (A), fluconazole (100 μg/ml) (B), trifluoperazine (1.3 mM) (C), or amphotericin B (200 μg/ml) (D). Each curve is plotted against control larvae injected with live or heat-killed (HK) spores germinated for 6 h and resuspended in PBS. p-values represent Log-rank test on live-treated vs. live-untreated spores.

https://doi.org/10.1371/journal.pone.0201915.g005

other fungal pathogens in *G. mellonella* [20], although the length of the infection required for killing by *P. destructans* is considerably longer. Experiments using heat-killed *P. destructans* spores, histology of larval tissue and recovery of fungal cells from infected larvae reveal that larval killing requires active fungal proliferation and is not simply a consequence of collateral damage from the host response to the inoculum. This is relevant as dead spores from some fungal species can kill larvae even in the absence of a live infection [35]. Together, these findings support the use of *G. mellonella* larvae as an accessible system for studying pathogenicity during *P. destructans* infection.

We found that pre-germination of *P. destructans* spores enhanced virulence levels, as spores germinated for 24 hours prior to infection were able to kill larvae ~3–4 times faster than non-germinated spores. There may be several non-mutually exclusive factors contributing to this phenomenon. One possibility is that spore germination does not readily occur within the larvae, so that pre-germinated spores exhibit an advantage as they have progressed past this rate-

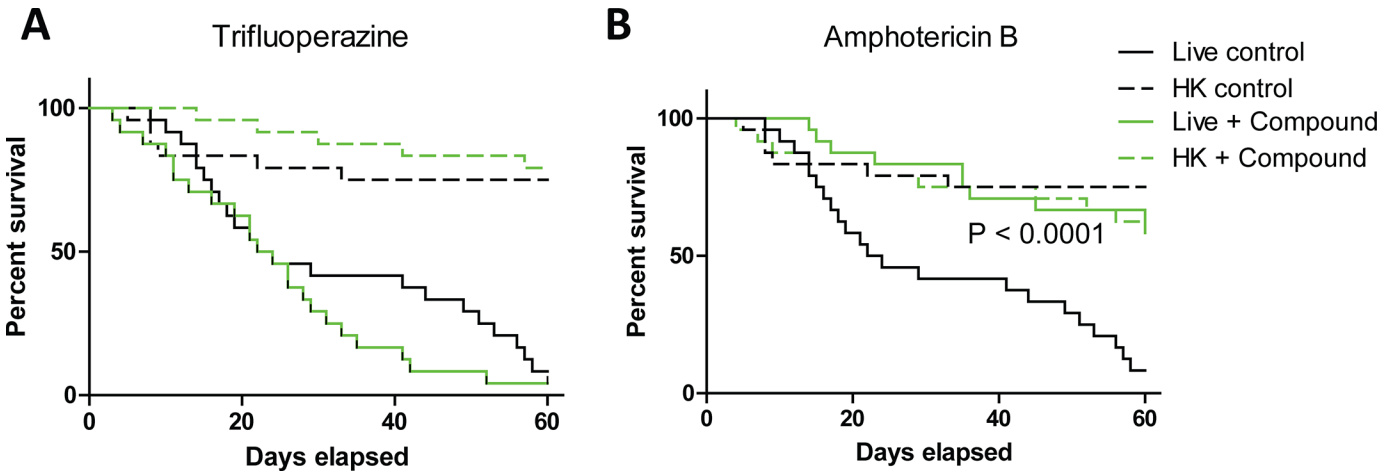

Fig 6. Evaluation of antifungal treatments administered after infection with *P. destructans*. Survival curves from *Galleria* larvae injected with spores (10^6/larva) and treated 2 hours later with trifluoperazine (1.3 mM) (A) or amphotericin B (200 μg/mL) (B). Each curve is plotted against control larvae injected with live or heat-killed (HK) spores which received a second injection of PBS alone. p-value represent Log-rank test on live + amphotericin B vs. live-untreated spores.

https://doi.org/10.1371/journal.pone.0201915.g006

limiting step. Alternatively, germinated spores could be more resistant to phagocytosis or other immune defenses than non-germinated spores. In line with this, cell shape and/or size has been shown to determine interactions between some fungal species and immune cells, with elongated hyphal cells being more resistant to phagocytosis than smaller yeast cells [36]. *P. destructans* spores that have initiated hyphae formation may therefore present a greater challenge to clearance by larval hemocytes. Remodeling of the fungal cell wall during spore germination may also impact immune responses. *C. albicans* hyphal cells, but not yeast cells, can block phagosome maturation and induce macrophage lysis due to expression of hyphal-specific cell wall components [37, 38]. It is possible that a similar mechanism allows germinated *P. destructans* spores to resist *G. mellonella* hemocytes, thereby accelerating infection. On the other hand, conidia from *Aspergillus fumigatus* possess hydrophobins [39] and melanins [40] that mask immunogenic components of the cell wall. Upon germination, *A. fumigatus* cells shed these components exposing surfaces that stimulate immune cell activation. The increased melanization of larvae injected with germinated spores suggests that *P. destructans* germ tubes may similarly stimulate a stronger immune response than non-germinated spores. However, given that germinated *P. destructans* spores are more virulent than non-germinated spores, this increased response is not protective and could even be detrimental to long-term survival in this model.

In addition to establishing conditions for infection of *G. mellonella* with *P. destructans*, we also used this model to test whether inhibitors of fungal growth could improve infection outcomes. A screen using Biolog PM plates identified 42 compounds that inhibited *P. destructans in vitro*, with effective inhibitors significantly enriched in compounds targeting the cell membrane and efflux pumps. A comparison with *C. albicans* [31] indicated that this species is similarly sensitive to these classes of inhibitors, although differences in growth conditions make it difficult to compare inhibitor responses between fungal species. We note that Chaturvedi *et al.* previously performed a more extensive screen of 1,920 compounds of which 1.4% were highly effective at inhibiting *P. destructans* growth, including several azole drugs, a fungicide (phenylmercuric acetate), as well as several biocides [10]. The fraction of effective compounds identified was similar to that of high-throughput screens for compounds against other fungal species, whereas the high hit rate in our more limited screen (35%) is presumably due to Biolog compounds having been pre-selected for those with potential antifungal activity.

We subsequently focused our analysis on trifluoperazine and sodium thiosulfate from the Biolog screen. Trifluoperazine is an antipsychotic drug that has been shown to have antimicrobial properties against a wide range of fungal and bacterial species [41, 42], whereas sodium thiosulfate has been used as a topical treatment for fungal infections [43]. We compared these inhibitors with two well-established antifungal drugs, fluconazole and amphotericin B, the latter of which was also an effective inhibitor of *P. destructans* growth in our screen. Of these four compounds, trifluoperazine and amphotericin B effectively blocked larval killing by *P. destructans* when applied prior to infection, yet only amphotericin B was effective when used post infection. The ineffectiveness of trifluoperazine post infection could be due to metabolism of the compound by *G. mellonella* or an inability of the drug to access sites of *P. destructans* infection. However, this compound could still have value as a preventative disinfectant as spores exposed to trifluoperazine for 2 h were rendered completely avirulent. Both trifluoperazine and amphotericin B are fungicidal (our data and [44]), suggesting this mode of action may be most effective for treatment of this fungus. Curiously, trifluoperazine was also tested as part of the Chaturvedi *et al*. screen but was not found to inhibit *P. destructans* growth [10], possibly due to differences in drug concentrations or culture conditions. The use of fungicidal drugs would also be beneficial for treatment of WNS in nature, as delivery of a single application to hibernating bat populations would be considerably more practical than multiple applications. The *G. mellonella* model can therefore enable screening of anti-*P. destructans* compounds and may help accelerate the development of an effective WNS treatment.

Finally, we note that the *G. mellonella* model also has limitations that should be considered. First, WNS is a mammalian disease in which infection follows the invasion of external dermal tissues, whereas *Galleria* is an invertebrate species where fungal spores are directly introduced into the insect hemolymph. The larval model therefore lacks important features that occur during fungal colonization and invasion of dermal tissues. Second, *G. mellonella*, like all insects, lacks an adaptive immune system. However, this difference may not be critical for modeling *P. destructans* infections, as overall immune function is down-regulated in hibernating animals [45], and adaptive immune responses are particularly lacking in hibernating bats, whereas innate pro-inflammatory signaling is activated in response to *P. destructans* [26–28]. Neutrophils are also present in hibernating bats [27, 28, 46], although neutrophil recruitment and activation by *P. destructans* may primarily occur upon a return to euthermia [47]. A number key aspects of innate immunity are, in fact, shared between *G. mellonella* and mammals, including pathogen-associated molecular pattern (PAMP) receptors, anti-microbial peptides and phagocytic cells [20]. *Galleria* hemocytes share similarities with mammalian neutrophils and can phagocytose microbes, generate reactive oxygen species (ROS) and produce extracellular net-like structures for microbial killing [23–25]. The *G. mellonella* immune system, while lacking adaptive immunity, therefore shows parallels to that of the natural host for *P. destructans*.

In conclusion, we demonstrate that *G. mellonella* represents a highly accessible model for the analysis of *P. destructans*, the primary cause of WNS. While there are limitations to this model its simplicity, ease of use, and affordability make it an attractive system for high-throughput screening of antifungal agents, as well as for the analysis of fungal mutants that may be defective in virulence. We suggest its inclusion will add to the growing list of tools available for the study of this emerging mammalian pathogen.

Supporting information

S1 Table. Biolog drug screen compounds. A full list of compounds included in the Biolog drug panel. Column headers indicate the following metadata from left to right: Plate ID, Well

ID, chemical name, mode of action (moa), Kegg database compound ID (co_id) and average activity index of *P. destructans* calculated using DuctApe software (avg activity).
(XLSX)

Acknowledgments

We would like to thank Iuliana Ene for assistance with PM data analysis, Corey Frazer and Iuliana Ene for comments on the paper, and Matthew Anderson and Matthew Hirakawa for help with larval injections.

Author Contributions

Conceptualization: Chapman N. Beekman, Richard J. Bennett.

Formal analysis: Chapman N. Beekman.

Funding acquisition: Richard J. Bennett.

Investigation: Chapman N. Beekman, Lauren Meckler, Eleanor Kim.

Methodology: Chapman N. Beekman.

Project administration: Richard J. Bennett.

Supervision: Chapman N. Beekman, Richard J. Bennett.

Writing – original draft: Chapman N. Beekman, Richard J. Bennett.

References

1. White-Nose Syndrome Fact Sheet. US Fish and Wildlife Service. April 2018.
2. Boyles JG, Cryan PM, McCracken GF, Kunz TH. Economic importance of bats in agriculture. Science. 2011; 332:2. https://doi.org/10.1126/science.1201366 PMID: 21454775.
3. Flieger M, Bandouchova H, Cerny J, Chudickova M, Kolarik M, Kovacova V, et al. Vitamin B2 as a virulence factor in *Pseudogymnoascus destructans* skin infection. Sci Rep. 2016; 6:33200. https://doi.org/10.1038/srep33200 PMID: 27620349; PubMed Central PMCID: PMC5020413.
4. Pannkuk EL, Risch TS, Savary BJ. Isolation and identification of an extracellular subtilisin-like serine protease secreted by the bat pathogen *Pseudogymnoascus destructans*. PLoS One. 2015; 10(3): e0120508. https://doi.org/10.1371/journal.pone.0120508 PMID: 25785714; PubMed Central PMCID: PMC4364704.
5. O'Donoghue AJ, Knudsen GM, Beekman C, Perry JA, Johnson AD, DeRisi JL, Craik CS, and Bennett RJ. Destructin-1 is a collagen-degrading endopeptidase secreted by *Pseudogymnoascus destructans*, the causative agent of white-nose syndrome. Proc Natl Acad Sci U S A. 2015; 112(24):E3152. https://doi.org/10.1073/pnas.1509071112 PMID: 26015578; PubMed Central PMCID: PMC4475950.
6. Frank CL, Ingala MR, Ravenelle RE, Dougherty-Howard K, Wicks SO, Herzog C, et al. The effects of cutaneous fatty acids on the growth of *Pseudogymnoascus destructans*, the etiological agent of white-nose syndrome (WNS). PLoS One. 2016; 11(4):e0153535. https://doi.org/10.1371/journal.pone.0153535 PMID: 27070905; PubMed Central PMCID: PMC4829186.
7. Reeder SM, Palmer JM, Prokkola JM, Lilley TM, Reeder DM, Field KA. *Pseudogymnoascus destructans* transcriptome changes during white-nose syndrome infections. Virulence. 2017:1–13. https://doi.org/10.1080/21505594.2017.1342910 PMID: 28614673.
8. Warnecke L, Turner JM, Bollinger TK, Lorch JM, Misra V, Cryan PM, et al. Inoculation of bats with European *Geomyces destructans* supports the novel pathogen hypothesis for the origin of white-nose syndrome. Proc Natl Acad Sci U S A. 2012; 109(18):6999–7003. https://doi.org/10.1073/pnas.1200374109 PMID: 22493237; PubMed Central PMCID: PMC3344949.
9. Lorch JM, Meteyer CU, Behr MJ, Boyles JG, Cryan PM, Hicks AC, et al. Experimental infection of bats with *Geomyces destructans* causes white-nose syndrome. Nature. 2011; 480(7377):376–8. https://doi.org/10.1038/nature10590 PMID: 22031324.
10. Chaturvedi S, Rajkumar SS, Li X, Hurteau GJ, Shtutman M, Chaturvedi V. Antifungal testing and high-throughput screening of compound library against *Geomyces destructans*, the etiologic agent of

geomycosis (WNS) in bats. PLoS One. 2011; 6(3):e17032. https://doi.org/10.1371/journal.pone.0017032 PMID: 21399675; PubMed Central PMCID: PMC3047530.

11. Wilson MB, Held BW, Freiborg AH, Blanchette RA, Salomon CE. Resource capture and competitive ability of non-pathogenic *Pseudogymnoascus spp.* and *P. destructans*, the cause of white-nose syndrome in bats. PLoS One. 2017; 12(6):e0178968. https://doi.org/10.1371/journal.pone.0178968 PMID: 28617823; PubMed Central PMCID: PMC5472292.
12. Cornelison CT, Keel K, Gabriel KT, Barlament CK, Tucker TA, Pierce GE, Crow SA Jr. A preliminary report on the contact-independent antagonism of *Pseudogymnoascus destructans* by *Rhodococcus rhodochrous* strain DAP96253. BMC Microbiology. 2014; 14(246). PubMed Central PMCID: PMC4181622.
13. Ene IV, Heilmann CJ, Sorgo AG, Walker LA, de Koster CG, Munro CA, et al. Carbon source-induced reprogramming of the cell wall proteome and secretome modulates the adherence and drug resistance of the fungal pathogen *Candida albicans*. Proteomics. 2012; 12(21):3164–79. https://doi.org/10.1002/pmic.201200228 PMID: 22997008; PubMed Central PMCID: PMC3569869.
14. Ene IV, Adya AK, Wehmeier S, Brand AC, MacCallum DM, Gow NA, et al. Host carbon sources modulate cell wall architecture, drug resistance and virulence in a fungal pathogen. Cell Microbiol. 2012; 14(9):1319–35. https://doi.org/10.1111/j.1462-5822.2012.01813.x PMID: 22587014; PubMed Central PMCID: PMC3465787.
15. Brennan M TD, Whiteway M, Kavanagh K,. Correlation between virulence of *Candida albicans* mutants in mice and *Galleria mellonella* larvae. FEMS Immunology and Medical Microbiology. 2002; 34:5. PMID: 12381467.
16. Li DD, Deng L, Hu GH, Zhao LX, Hu DD, Jiang YY, Wang Y. Using *Galleria mellonella–Candida albicans* infection model to evaluate antifungal agents. Biol Pharm Bull. 2013; 36(9):1482–7. PubMed Central PMCID: PMC23995660. PMID: 23995660
17. Mesa-Arango AC, Forastiero A, Bernal-Martinez L, Cuenca-Estrella M, Mellado E, Zaragoza O. The non-mammalian host *Galleria mellonella* can be used to study the virulence of the fungal pathogen *Candida tropicalis* and the efficacy of antifungal drugs during infection by this pathogenic yeast. Med Mycol. 2013; 51(5):461–72. https://doi.org/10.3109/13693786.2012.737031 PMID: 23170962.
18. Maurer E, Browne N, Surlis C, Jukic E, Moser P, Kavanagh K, et al. *Galleria mellonella* as a host model to study *Aspergillus terreus* virulence and amphotericin B resistance. Virulence. 2015; 6(6):591–8. https://doi.org/10.1080/21505594.2015.1045183 PMID: 26107350; PubMed Central PMCID: PMC4720272.
19. Slater JL, Gregson L, Denning DW, Warn PA. Pathogenicity of *Aspergillus fumigatus* mutants assessed in *Galleria mellonella* matches that in mice. Med Mycol. 2011; 49 Suppl 1:S107–13. https://doi.org/10.3109/13693786.2010.523852 PMID: 20950221.
20. Binder U, Maurer E, Lass-Florl C. *Galleria mellonella*: An invertebrate model to study pathogenicity in correctly defined fungal species. Fungal Biol. 2016; 120(2):288–95. https://doi.org/10.1016/j.funbio.2015.06.002 PMID: 26781383.
21. Coleman JJ, Muhammed M, Kasperkovitz PV, Vyas JM, Mylonakis E. *Fusarium* pathogenesis investigated using *Galleria mellonella* as a heterologous host. Fungal Biol. 2011; 115(12):1279–89. https://doi.org/10.1016/j.funbio.2011.09.005 PMID: 22115447; PubMed Central PMCID: PMC3224342.
22. Garcia-Rodas R, Casadevall A, Rodriguez-Tudela JL, Cuenca-Estrella M, Zaragoza O. *Cryptococcus neoformans* capsular enlargement and cellular gigantism during *Galleria mellonella* infection. PLoS One. 2011; 6(9):e24485. https://doi.org/10.1371/journal.pone.0024485 PMID: 21915338; PubMed Central PMCID: PMC3168503.
23. Browne N, Heelan M, Kavanagh K. An analysis of the structural and functional similarities of insect hemocytes and mammalian phagocytes. Virulence. 2013; 4(7):597–603. https://doi.org/10.4161/viru.25906 PMID: 23921374; PubMed Central PMCID: PMC3906293.
24. Bergin D, Reeves EP, Renwick J, Wientjes FB, Kavanagh K. Superoxide production in *Galleria mellonella* hemocytes: identification of proteins homologous to the NADPH oxidase complex of human neutrophils. Infect Immun. 2005; 73(7):4161–70. https://doi.org/10.1128/IAI.73.7.4161-4170.2005 PMID: 15972506; PubMed Central PMCID: PMC1168619.
25. Renwick J, Reeves EP, Wientjes FB, Kavanagh K. Translocation of proteins homologous to human neutrophil $p47^{phox}$ and $p67^{phox}$ to the cell membrane in activated hemocytes of *Galleria mellonella*. Dev Comp Immunol. 2007; 31(4):347–59. https://doi.org/10.1016/j.dci.2006.06.007 PMID: 16920193.
26. Rapin N, Johns K, Martin L, Warnecke L, Turner JM, Bollinger TK, et al. Activation of innate immune-response genes in little brown bats (*Myotis lucifugus*) infected with the fungus *Pseudogymnoascus destructans*. PLoS One. 2014; 9(11):e112285. https://doi.org/10.1371/journal.pone.0112285 PMID: 25391018; PubMed Central PMCID: PMC4229191.

27. Moore MS, Reichard JD, Murtha TD, Nabhan ML, Pian RE, Ferreira JS, et al. Hibernating little brown myotis (*Myotis lucifugus*) show variable immunological responses to white-nose syndrome. PLoS One. 2013; 8(3):e58976. https://doi.org/10.1371/journal.pone.0058976 PMID: 23527062; PubMed Central PMCID: PMC3604015.

28. Field KA, Johnson JS, Lilley TM, Reeder SM, Rogers EJ, Behr MJ, et al. The white-nose syndrome transcriptome: activation of anti-fungal host responses in wing tissue of hibernating little brown *Myotis*. PLoS Pathog. 2015; 11(10):e1005168. https://doi.org/10.1371/journal.ppat.1005168 PMID: 26426272; PubMed Central PMCID: PMC4591128.

29. Bochner BR, Gadzinski P, Panomitros E. Phenotype microarrays for high-throughput phenotypic testing and assay of gene function. Genome Res. 2001; 11:1246–55. https://doi.org/10.1101/gr.186501 PMID: 11435407; PubMed Central PMCID: PMC155265.

30. Galardini M, Mengoni A, Biondi EG, Semeraro R, Florio A, Bazzicalupo M, et al. DuctApe: a suite for the analysis and correlation of genomic and OmniLog Phenotype Microarray data. Genomics. 2014; 103 (1):1–10. https://doi.org/10.1016/j.ygeno.2013.11.005 PMID: 24316132.

31. Ene IV, Lohse MB, Vladu AV, Morschhauser J, Johnson AD, Bennett RJ. Phenotypic profiling reveals that *Candida albicans* opaque cells represent a metabolically specialized cell state compared to default white cells. MBio. 2016; 7(6). https://doi.org/10.1128/mBio.01269-16 PMID: 27879329; PubMed Central PMCID: PMC5120136.

32. Hulsen T, de Vlieg J, Alkema W. BioVenn—a web application for the comparison and visualization of biological lists using area-proportional Venn diagrams. BMC Genomics. 2008; 9:488. https://doi.org/10.1186/1471-2164-9-488 PMID: 18925949; PubMed Central PMCID: PMC2584113.

33. Pye AE. Activation of prophenoloxidase and inhibition of melanization in the haemolymph of immune *Galleria mellonella* larvae. Insect Biochemistry. 1977; 8:7.

34. Cowen LE. The evolution of fungal drug resistance: modulating the trajectory from genotype to phenotype. Nat Rev Microbiol. 2008; 6(3):187–98. Epub 2008/02/05. doi: nrmicro1835 [pii] https://doi.org/10.1038/nrmicro1835 PMID: 18246082.

35. Achterman RR, Smith AR, Oliver BG, White TC. Sequenced dermatophyte strains: growth rate, conidiation, drug susceptibilities, and virulence in an invertebrate model. Fungal Genet Biol. 2011; 48(3):335–41. https://doi.org/10.1016/j.fgb.2010.11.010 PMID: 21145410; PubMed Central PMCID: PMC3035951.

36. Erwig LP, Gow NA. Interactions of fungal pathogens with phagocytes. Nat Rev Microbiol. 2016; 14 (3):163–76. https://doi.org/10.1038/nrmicro.2015.21 PMID: 26853116.

37. Uwamahoro N, Verma-Gaur J, Shen HH, Qu Y, Lewis R, Lu J, et al. The pathogen *Candida albicans* hijacks pyroptosis for escape from macrophages. MBio. 2014; 5(2):e00003–14. https://doi.org/10.1128/mBio.00003-14 PMID: 24667705; PubMed Central PMCID: PMC3977349.

38. Bain JM, Louw J, Lewis LE, Okai B, Walls CA, Ballou ER, et al. *Candida albicans* hypha formation and mannan masking of beta-glucan inhibit macrophage phagosome maturation. MBio. 2014; 5(6):e01874. https://doi.org/10.1128/mBio.01874-14 PMID: 25467440; PubMed Central PMCID: PMC4324242.

39. Aimanianda V, Bayry J, Bozza S, Kniemeyer O, Perruccio K, Elluru SR, et al. Surface hydrophobin prevents immune recognition of airborne fungal spores. Nature. 2009; 460(7259):1117–21. https://doi.org/10.1038/nature08264 PMID: 19713928.

40. Chai LY, Netea MG, Sugui J, Vonk AG, van de Sande WW, Warris A, et al. *Aspergillus fumigatus* conidial melanin modulates host cytokine response. Immunobiology. 2010; 215(11):915–20. https://doi.org/10.1016/j.imbio.2009.10.002 PMID: 19939494; PubMed Central PMCID: PMC2891869.

41. Eilam Y, Polacheck I, Ben-Gigi G, Chernichovsky D. Activity of phenothiazines against medically important yeasts. Antimicrob Agents Chemother. 1987; 31(5):834–6. PMID: 3300543; PubMed Central PMCID: PMC174848.

42. Vitale RG, Afeltra J, Meis JF, Verweij PE. Activity and post antifungal effect of chlorpromazine and trifluopherazine against *Aspergillus*, *Scedosporium* and zygomycetes. Mycoses. 2007; 50(4):270–6. https://doi.org/10.1111/j.1439-0507.2007.01371.x PMID: 17576318.

43. Rezabek. Superficial fungal infections of the skin. Diagnosis and current treatment recommendations. Drugs (New York, NY). 1992; 43(5):674–82.

44. Anderson TM, Clay MC, Cioffi AG, Diaz KA, Hisao GS, Tuttle MD, et al. Amphotericin forms an extramembranous and fungicidal sterol sponge. Nat Chem Biol. 2014; 10(5):400–6. https://doi.org/10.1038/nchembio.1496 PMID: 24681535; PubMed Central PMCID: PMC3992202.

45. Bouma H. Hibernation: the immune system at rest? J Leukoc Biol. 2010; 88(4):619. https://doi.org/10.1189/jlb.0310174 PMID: 20519639.

46. Meteyer CU, Valent M, Kashmer J, Buckles EL, Lorch JM, Blehert DS, et al. Recovery of little brown bats (*Myotis lucifugus*) from natural infection with *Geomyces destructans*, white-nose syndrome. J Wildl Dis. 2011; 47(3):618–26. https://doi.org/10.7589/0090-3558-47.3.618 PMID: 21719826.

47. Meteyer CU, Barber D, Mandl JN. Pathology in euthermic bats with white nose syndrome suggests a natural manifestation of immune reconstitution inflammatory syndrome. Virulence. 2012; 3(7):583–8. https://doi.org/10.4161/viru.22330 PMID: 23154286; PubMed Central PMCID: PMC3545935.